Directivity-Reconfigurable Wideband Two-Arm Spiral Antenna

Peng Liu, Siming Yang, Xinran Wang, Mingda Yang, Jiming Song, and Liang Dong

***Abstract*—This letter reports a novel directivity-reconfigurable wideband antenna in microwave regime. The antenna is formed by encasing liquid metal alloys into a highly stretchable elastomer. A two-arm Archimedean spiral antenna is adopted to implement the concept of optimizing directivity by inflating the elastomer to form a dome-shaped antenna. Microelectromechanical system-based microblowers are employed to pneumatically control the shape of the antenna. The antenna can operate in a wide frequency band from 6.9 to 13.8 GHz. The ability to change the shape of the antenna allows optimizing its radiation pattern by making it more directive in the inflation direction, while its passing band remains wide. The antenna also provides good circular polarization of an electromagnetic wave.**

***Index Terms*—Directivity, flexible electronics, microelectromechanical systems (MEMS), reconfigurable, wideband antenna.**

I. Introduction

FLEXIBLE electronics have been extensively studied because they provide a simple means of integrating electronic devices on curved surfaces for various applications, such as wearable devices, artificial skins, flexible displays, and flexible solar energy harvesters [1]–[6]. Recently, inclusion of liquid metal into a flexible elastomer has led to several tunable electronic and electromagnetic devices, including electrical probes [7], microfluidic electrodes [8], electrical interconnectors [9], antennas [10]–[12], and metamaterials [13]. Liquid metal can flow and reshape when responding to mechanical deformation without cracking or fatigue. Among many liquid metals and alloys, gallium–indium eutectic (EGaIn) is considered as a promising metallization candidate for flexible electronics because of its liquid state in room temperature and low toxicity compared to mercury. Using this liquid metal alloy, we have recently developed stretchable and tunable microwave meta-atoms [13] and meta-skins for tunable frequency selective surface and invisibility cloak applications [14], where an array of EGaIn split-ring resonators are embedded inside a silicone elastomer.

Reconfigurable antennas have attracted increasing attention due to the explosive growth of wireless communications, satellite communications, wireless power transfer, radar, etc., where radiation pattern reconfigurability of antennas is highly demanded. Several liquid-metal-based tunable antennas have been reported based on different tuning mechanisms and designs, including a stretchable dipole antenna or unbalanced loop antenna [15], an electrically small antenna [16], and an electrochemical controlled capillary actuated monopole antenna [12]. All of these reconfigurable antennas are mainly focused on frequency tuning and exhibit their radiation patterns with relatively low directivity. It should be noted that directional antennas are challenging to develop and are widely demanded for applications such as wireless communication, remote sensing, and targeted power transfer. Therefore, antennas capable of reconfiguring directivity are highly desired to optimize their transmission or receiving power in a specific direction of interest.

In this letter, we report the development of a directivity-reconfigurable two-arm spiral antenna made of all flexible materials. The original planar antenna can be inflated to form a dome-like shape by blowing high-pressure air into an air cavity below the antenna with the help of a commercial microelectromechanical systems (MEMS)-based microblowers. The ability to change the shape of the antenna allows reconfiguring the radiation pattern of the antenna along the main lobe direction or the inflation direction. Due to the formation of the dome-shaped structure, the radiation pattern of the antenna becomes sharper, thus optimizing its directivity, while its passing band still remains in a wide frequency range. Also, the present antenna provides good circular polarization.

II. Design and Fabrication

Fig. 1(a) shows schematic for a planar self-complementary, two-arm Archimedean spiral antenna made of liquid metal encased by a stretchable silicone elastomer. The operating frequency range of the antenna can be determined by the innermost radius a and the outermost radius b. In order to operate in X-band regime, the antenna is designed to have $a = 3.5$ mm and $b = 18.5$ mm. Each spiral arm has 2.5 turns. The width of the liquid metal is $w = 1.5$ mm, and the gap between two arms is $g = 1.5$ mm.

Fig. 1(c) shows the fabrication process for the antenna. First, an SU-8 photoresist (Microchem, Westborough, MA) is patterned with the designed spirals on a silicon wafer W1. Subsequently, a 700-μm-thick silicone layer L1 is formed by casting a prepolymer solution of silicone Ecoflex (Smooth-On, Macungie, PA) on the SU-8 mold, followed by a thermal curing process at 60 °C on a hotplate for 30 min. The fully cured L1 layer is then peeled from the SU-8 mold with the spiral channels inside it. To inject the liquid metal alloy EGaIn into the channels, an inlet and an outlet are mechanically punched at the two ends of each channel. Due to the natural poor adhesion

Manuscript received January 21, 2016; revised March 22, 2016; accepted April 17, 2016. Date of publication April 21, 2016; date of current version February 13, 2017. This work was supported in part by the U.S. National Science Foundation under Grant # ECCS-0954765 and China Scholarship Council. P. Liu and S. Yang contributed equally to this work

The authors are with the Department of Electrical and Computer Engineering, Iowa State University, Ames, IA 50011 USA (e-mail: pengliu@iastate.edu; ysm@iastate.edu; xrwang@iastate.edu; mingda@iastate.edu; jisong@iastate.edu; ldong@iastate.edu).

Color versions of one or more of the figures in this letter are available online at http://ieeexplore.ieee.org.

Digital Object Identifier 10.1109/LAWP.2016.2555941

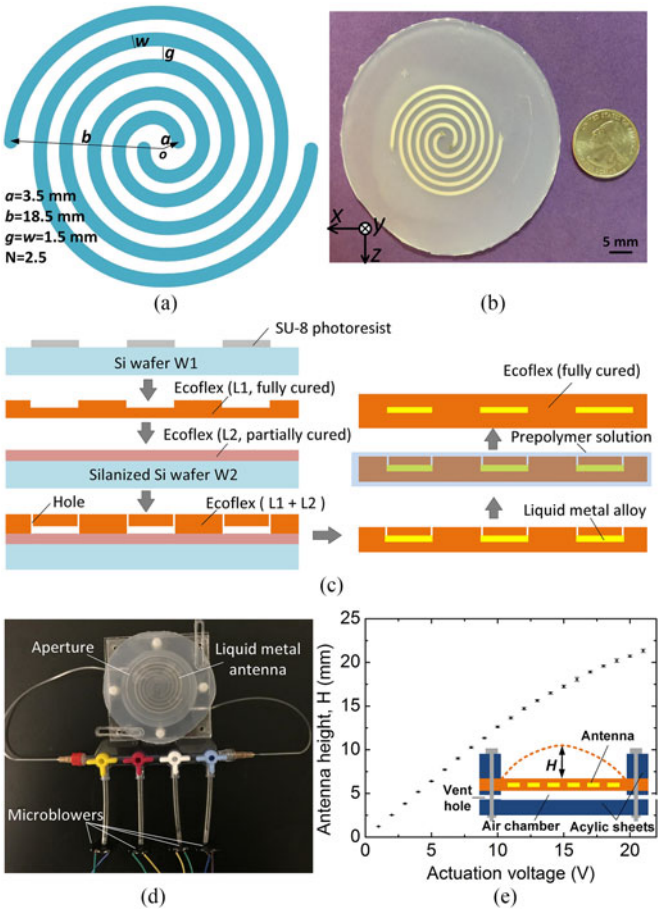

Fig. 1. (a) Design parameters of the proposed two-arm spiral antenna. (b) Photograph of the fabricated planar antenna before assembled to a pneumatic control unit. (c) Schematic of the fabrication process for the planar antenna. (d) Photograph of the assembled directivity reconfigurable antenna with a pneumatic air control unit or four voltage-controlled MEMS microblowers. (e) Measured relationship between the inflation height H and the actuation dc voltage applied to the microblowers. The error bars represent standard deviations obtained via 100 times repeatability measurements.

between fully cured Ecoflex, a 100-μm-thick Ecoflex layer L2 is partially cured on a silanized bare Si wafer W2 at 45 °C for 40 s. After that, the fully cured L1 and the partially cured L2 are immediately transferred to a hotplate at 90 °C for 20 min. This allows permanently bonding the two layers. Thus, the spiral channels are formed inside the elastomer. After EGaIn is manually injected into the channels with a metal needle (#20 Gauge) amounted on a syringe (10 mL; Becton-Dickinson, Franklin Lakes, NJ), the residues of liquid metal left around the inlets and outlets are cleaned by a cotton swab dipped with a hydrochloric acid solution (50%, v/v). Finally, the device is immersed into a thin prepolymer solution of Ecoflex and then is fully cured at 80°C for 30 min to seal the inlets and outlets. The total thickness of the elastomer is approximately 1 mm. The liquid metal is located in nearly half the thickness of the elastomer [see Fig. 1(b) and (c)].

In order to deform the liquid metal antenna and control its deformation, an inexpensive and accurate control unit is built with MEMS microblowers (MZB1001E00; Murata, Kyoto, Japan). Briefly, the microblower utilizes a piezoelectric-based drive method that features small dimensions and is suitable as a source

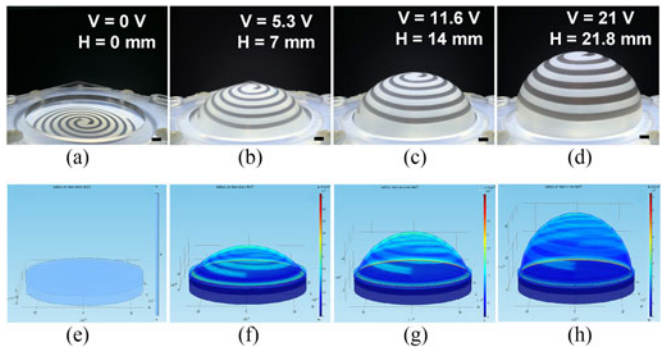

Fig. 2. (a)–(d) Time-lapse images and (e)–(h) FEA simulation results for the Ecoflex elastomer containing the liquid metal antenna with different inflation heights: (a), (e) 0 mm; (b), (f) 7 mm; (c), (g) 14 mm; and (d), (h) 21.8 mm. Scale bars in (a)–(d) represent 3 mm.

for high-pressure air generation with compact and low profile. To provide a high pressure to deform the antenna, four microblowers are connected in parallel with tubing and three-way hose fittings [see Fig. 1(d)]. Subsequently, the planar antenna is sandwiched between two 3-mm-thick acrylic boards (Total Plastic, Baltimore, MD) and fixed by four nylon mechanical cap screws. The lower acrylic board is premachined to form a 1-mm-deep cavity and two lateral air vents. A circular through-hole with the diameter of 50 mm is created in the upper cladding board. When a dc voltage is applied to the microblowers, the microblowers generate high-speed airflow to pneumatically push the elastomer into a dome-like cap.

III. Results and Discussion

First, the relationship between the applied actuation dc voltage to the microblowers and the resulting height H is investigated. As shown in Fig. 1(e), H increases almost linearly with an applied voltage at low-voltage regions (0–10 V) and then increases slightly slowly at high-voltage regions (11–12 V). At the maximum allowed voltage of 21 V for the microblowers, the obtained dome height is 21.8 mm. The shape change repeatability of the antenna is investigated by inflating and deflating the antenna for 100 times. The obtained standard deviation of inflation height is less than 1.5%, indicating a good repeatability and reliability of this actuation method. During the repeatability test, the liquid metal inside the spiral channels dynamically responds to the applied pressures by changing its shape and dimensions. No fatigue or cracking is found with the liquid metal or Ecoflex after the repeatability measurements. It takes about 6.5 s for the microblowers to inflate the planar antenna from flat to the maximum dome height of 21.8 mm at 21 V. By increasing the number of the microblowers or exploring other actuation mechanisms, the actuation time of the device can be reduced.

Fig. 2 shows the mechanical simulation for four instances of the antenna under different actuation voltages applied to the microblowers. The simulation is performed using finite element analysis method-based software (COMSOL). Young's modulus and Poisson's ratio of Ecoflex are 29.5 kPa and 0.43, respectively. The pressure values for the simulation are obtained by using a pressure sensor (SPD015AA; Smartec, The Netherlands). As the Ecoflex membrane is inflated, mechanical restoring force of the elastomer acts to balance with the increased internal air

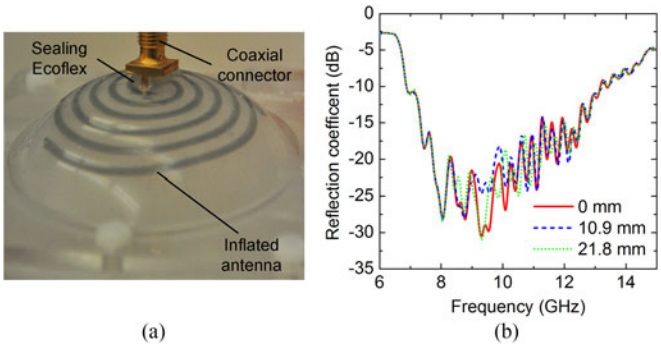

Fig. 3. (a) Photograph of the liquid metal antenna with a feeding structure. (b) Measured reflection coefficient for different inflation heights of the antenna.

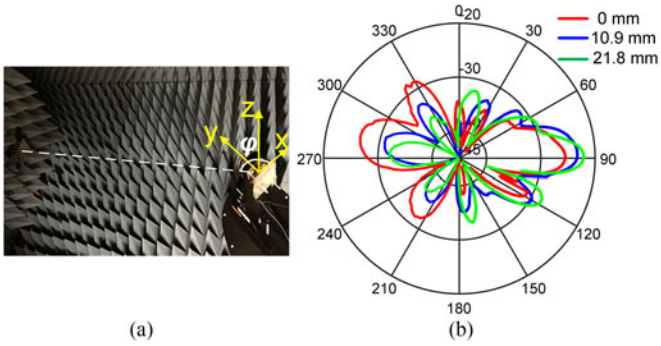

Fig. 4. (a) Measurement setup for measuring the radiation pattern of the liquid metal antenna with horizontal polarization. (b) Measured radiation pattern at 8.5 GHz of horizontal polarization for three inflation heights.

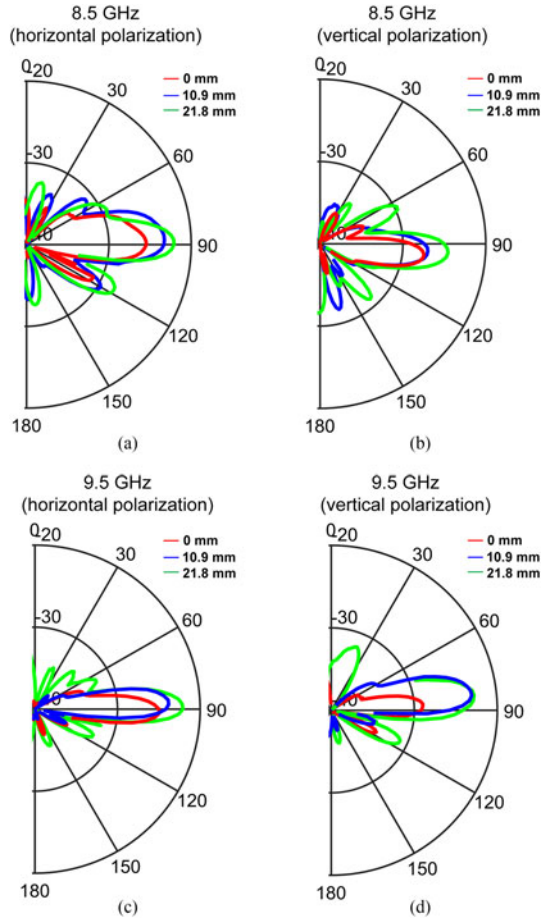

Fig. 5. Measured radiation patterns of both horizontal and vertical polarizations from 0° to 180° for different inflation heights at two sample frequencies: (a), (b) 8.5 GHz; and (c), (d) 9.5 GHz.

pressure, thus obtaining an equilibrium shape at a certain height of the dome. For $H = 0, 7, 14,$ and 21 mm under the applied pressure of 0, 2.2, 5.2, and 11.8 kPa, the resulting maximum surface stress in the deformed Ecoflex membrane is found to be 0, 184, 491, and 915 kN/m^2, respectively.

Next, electromagnetic measurement of the antenna is carried out in an anechoic chamber. The antenna is fed by input signals at the two heads of the spiral arms in the center region via a 3-mm SMA coaxial connector. The central pin and the ground pin of the connector are directly in contact with the liquid metal by inserting the two pins into the channels. A drop of Ecoflex precursor solution is added and then polymerized to seal the holes formed during the insertion [see Fig. 3(a)]. A coaxial cable is then connected to a programmable vector network analyzer (VNA, Agilent E8364). The reflection coefficient as a function of frequency for different dome heights is measured and plotted in Fig. 3(b). The result shows that as the antenna is inflated, the passing band for the antenna remains in a wide frequency range from 6.9 to 13.2 GHz with S_{11} lower than -10 dB.

The radiation pattern of the antenna is measured with a horn antenna in the far-field region using an automated antenna measurement system (Diamond Engineering, Diamond Springs, CA, USA) [see Fig. 4(a)]. The liquid metal antenna sits on a turntable rotating about z-axis and the dashed line extending from the horn antenna is in xy-plane. The rotation angle φ is defined as the angle between the horn antenna (dashed line) and x-axis. When $\varphi = 90°$, the inflated dome of the antenna points towards the horn antenna. At each angle, 21 measurements are performed to minimize the influence of possible mechanical errors.

Fig. 4(b) shows the radiation patterns of the antenna with horizontal polarization at 8.5 GHz for three different inflation heights: 0, 10.9, and 21.8 mm. The result indicates that the signal strength exhibits the strongest along the y-axis (here, y-direction at 90° and $-y$-direction at 270°). The flat liquid metal antenna transmits almost same signal strength for both y- and $-y$-directions because of the geometrical symmetry at xz-plane along y-axis. As the inflation height increases, the liquid metal antenna tends to increase the radiation along y-direction (90°), while decreasing the radiation along $-y$-direction (270°). Further increasing the inflation height will further enhance the radiation along y-direction. Therefore, the directivity at the main lobe direction (y-direction) can be optimized by inflating the antenna to higher heights.

The radiation patterns of the antenna at different frequencies are also measured in the frequency range from 7.6 to 9.8 GHz with the reflection power lower than -20 dB. Fig. 5 shows the normalized radiation patterns of the liquid metal antenna for three inflation heights (0, 10.9, and 21.8 mm) at two sample frequencies (8.5 and 9.5 GHz). By rotating the receiving horn antenna by 90°, the radiation patterns of vertical polarization are also measured.

TABLE I
DIRECTIVITY AND EFFICIENCY WITH DIFFERENT HEIGHTS AND FREQUENCIES

		Dome height		
	Frequency	0 mm	10.9 mm	21.8 mm
Directivity	8.5 GHz	5.39 dB	7.24 dB	7.74 dB
	9.5 GHz	7.57 dB	8.92 dB	9.90 dB
Efficiency	8.5 GHz	54.2%	46.4%	72%
	9.5 GHz	40%	45.1%	60.5%

TABLE II
AXIAL RATIO FOR DIFFERENT INFLATION HEIGHTS AND FREQUENCIES

	0 (mm)	10.9 (mm)	21.8 (mm)
8.5 GHz	1.25	1.54	1.32
9.5 GHz	1.58	1.10	1.08

As mentioned above, the directivity of the antenna can be improved only in the inflation direction of the dome. Consequently, the radiation patterns of the antenna are measured only from 0° to 180° along the main lobe direction or the inflation direction (90° in the radiation pattern plots). The measured radiation patterns show good directivity for all the measured heights at 8.5 and 9.5 GHz. With the measured radiation pattern, we can evaluate the directivity of this antenna (see Table I). The efficiency of the antenna varies between 40% and 72% for different inflation heights and frequencies.

More importantly, with increasing the inflation height, the antenna exhibits stronger directivity along its main lobe direction, thus optimizing its directivity along the inflation direction. Specifically, at 8.5 GHz, by inflating the antenna from 0 to 10.9 mm and further to 21.8 mm, the signal strength is improved by 2 dB and further to 3 dB in the horizontal polarization direction, and by 1 dB and further to 3 dB in the vertical polarization direction. Similarly, at 9.5 GHz, the signal strength in the inflation direction is also enhanced by 3 and 6 dB for the horizontal and vertical polarization, respectively. It should be pointed out that as the radiation pattern shows a good similarity between the vertical and horizontal polarizations, the antenna provides good circular polarization of an electromagnetic wave, and the axial ratio is shown in Table II.

Furthermore, benefiting from the deformability of the liquid metal and elastomer, the present antenna is able to preserve its electromagnetic properties after being inflated for 500 times to the maximum height of 21.8 mm.

Theoretically, the directivity of the device can be further enhanced by adding a back reflector or cavity. However, it is difficult to keep the gap distance unchanged between the antenna and the reflector during the mechanical deformation of the antenna. We will optimize the device and introduce a cavity to the design in the future. Nevertheless, the demonstrated reconfigurability of the present device allows for continuously tuning the radiation pattern and directivity of the antenna.

Lastly, to obtain the full benefit of structural tuning, the device needs to operate at temperatures that keep the infused liquid metal in a liquid state. EGaIn used in this letter has a melting point of $\sim 15.5\,^{\circ}\mathrm{C}$, making it liquid at room temperature [17]. It should be pointed out that when lower operation temperatures are needed, the device requires using other liquid metals or alloys with lower melting points.

IV. CONCLUSION

A liquid-metal-based antenna with a wide frequency band has been developed, and its capability to optimize directivity has been demonstrated. The antenna is formed by encasing EGaIn into Ecoflex elastomer and can withstand a large deformation with a good reliability and repeatability. This allows inflating the antenna containing elastomer to form a dome-like structure with different heights by pneumatically pumping high-pressure air into an air cavity using MEMS microblowers. By increasing the inflation height, the signal strength of the antenna can be improved to different extents. The antenna retains its wideband character without being affected by the pneumatic inflation. With an improved directivity in a broad operating frequency range, the antenna can radiate more energy toward the receiver. It is believed that the antenna can find its applications where targeted power transfer, high directivity, circular polarization, and wide operating frequency band are needed.

REFERENCES

[1] K. Hong, S. H. Kim, K. H. Lee, and C. D. Frisbie, "Printed, sub-2V ZnO electrolyte gated transistors and inverters on plastic," *Adv. Mater.*, vol. 25, no. 25, pp. 3413–3418, Jul. 2013.
[2] D. H. Kim *et al.*, "Stretchable and foldable silicon integrated circuits," *Science*, vol. 320, no. 5875, pp. 507–511, Apr. 2008.
[3] D. H. Kim *et al.*, "Optimized structural designs for stretchable silicon integrated circuits," *Small*, vol. 5, no. 24, pp. 2841–2847, Dec. 2009.
[4] J. H. So *et al.*, "Reversibly deformable and mechanically tunable fluidic antennas," *Adv. Funct. Mater.*, vol. 19, no. 22, pp. 3632–3637, Nov. 2009.
[5] W. Z. Wu, X. N. Wen, and Z. L. Wang, "Taxel-addressable matrix of vertical-nanowire piezotronic transistors for active and adaptive tactile imaging," *Science*, vol. 340, no. 6135, pp. 952–957, May 2013.
[6] J. Yoon *et al.*, "Design and fabrication of novel stretchable device arrays on a deformable polymer substrate with embedded liquid-metal interconnections," *Adv. Mater.*, vol. 26, no. 38, pp. 6580–6586, Oct. 2014.
[7] R. C. Chiechi, E. A. Weiss, M. D. Dickey, and G. M. Whitesides, "Eutectic gallium–indium (EGaIn): A moldable liquid metal for electrical characterization of self-assembled monolayers," *Angew. Chem. Int. Ed.*, vol. 47, no. 1, pp. 142–144, 2008.
[8] J.-H. So and M. D. Dickey, "Inherently aligned microfluidic electrodes composed of liquid metal," *Lab Chip*, vol. 11, no. 5, pp. 905–911, 2011.
[9] H. J. Kim, C. Son, and B. Ziaie, "A multiaxial stretchable interconnect using liquid-alloy-filled elastomeric microchannels," *Appl. Phys. Lett.*, vol. 92, Jan. 2008, Art. no. 011904.
[10] G. J. Hayes, J. H. So, A. Qusba, M. D. Dickey, and G. Lazzi, "Flexible liquid metal alloy (EGaIn) microstrip patch antenna," *IEEE Trans. Antennas Propag.*, vol. 60, no. 5, pp. 2151–2156, May 2012.
[11] M. Kubo *et al.*, "Stretchable microfluidic radiofrequency antennas," *Adv. Mater.*, vol. 22, no. 25, pp. 2749–2752, Jul. 2010.
[12] M. Wang, C. Trlica, M. R. Khan, M. D. Dickey, and J. J. Adams, "A reconfigurable liquid metal antenna driven by electrochemically controlled capillarity," *J. Appl. Phys.*, vol. 117, May 2015, Art. no. 194901.
[13] P. Liu *et al.*, "Tunable meta-atom using liquid metal embedded in stretchable polymer," *J. Appl. Phys.*, vol. 118, Jul. 2015, Art. no. 014504.
[14] S. Yang *et al.*, "From flexible and stretchable meta-atom to metamaterial: A wearable microwave meta-skin with tunable frequency selective and cloaking effects," *Sci. Rep.*, vol. 6, Feb 2016, Art. no. 21921.
[15] S. Cheng, A. Rydberg, K. Hjort, and Z. G. Wu, "Liquid metal stretchable unbalanced loop antenna," *Appl. Phys. Lett.*, vol. 94, Apr. 2009, Art. no. 144103.
[16] M. Jobs, K. Hjort, A. Rydberg, and Z. G. Wu, "A tunable spherical cap microfluidic electrically small antenna," *Small*, vol. 9, no. 19, pp. 3230–3234, Oct. 2013.
[17] M. D. Dickey *et al.*, "Eutectic gallium–indium (EGaIn): A liquid metal alloy for the formation of stable structures in microchannels at room temperature," *Adv. Funct. Mater.*, vol. 18, no. 7, pp. 1097–1104, Apr. 2008.